

# Annealing of preexisting defects in silicon single crystals by ion irradiation

M.D. Mihai<sup>a,b,\*</sup>, P. Ionescu<sup>a</sup>, D. Pantelica<sup>a</sup>, H. Petrascu<sup>a</sup>, D. Craciun<sup>c</sup>, V. Craciun<sup>c</sup>, F. Vasiliu<sup>d</sup>, B.S. Vasile<sup>b</sup>, I. Mercioniu<sup>d</sup>

<sup>a</sup> Horia Hulubei National Institute for Physics and Nuclear Engineering, P.O.B. MG-6, RO-077125, 30 Reactorului St., Magurele-Bucharest, Romania

<sup>b</sup> University Politehnica of Bucharest, RO 060042, Romania

<sup>c</sup> National Institute for Laser, Plasma and Radiation Physics, P.O.B. MG-36, RO-077125, 409 Atomistilor Str., Magurele-Bucharest, Romania

<sup>d</sup> National Institute of Materials Physics, P.O.B. MG-7, RO-077125, Atomistilor Str. 405A, Magurele-Bucharest, Romania

## ABSTRACT

The annealing of crystalline defects in Si single crystals created by ion implantation at room temperature was investigated. Silicon single crystals were firstly implanted at room temperature with 1.345 MeV Au<sup>1+</sup> ions at fluences from  $1 \times 10^{13}$  to  $1 \times 10^{14}$  at/cm<sup>2</sup> to induce damage. A second implantation at room temperature was afterwards performed with 10 MeV Co<sup>3+</sup> ions at a fluence of  $3 \times 10^{14}$  at/cm<sup>2</sup>. All samples were analyzed afterwards by Rutherford backscattering in random and channeling geometry to assess the crystalline damage present in the surface region. The results showed a significant reduction of the degree of damage or a reduction of the size of damaged region. The morphology and local atomic structure, studied using high-resolution electron microscopy, selected area electron diffraction and high resolution X-ray diffraction confirmed the reduction of damage degree and volume caused by Au implantation after Co implantation.

## 1. Introduction

Due to the early interest for the development of the ion implantation doping process in Si for microelectronics applications, previous studies were mainly focused on the irradiation with ions having energies in the range of a few hundreds of keV to a few MeV, i.e., in a slowing down regime where the nuclear energy loss is dominant. These investigations showed that Si is quite easily damaged at or below room temperature (RT) and that, depending on the ion fluence, the resulting damage takes the form of partial or total amorphization of the bombarded layer. Since this disorder is detrimental to device performance, many attempts were made to recover the original crystallinity [1–6].

One of the important methods to recover the original crystallinity is the solid phase epitaxy (SPE) technique [7,8]. In case of Si the annealing, temperatures greater than 823 K are generally needed for SPE process. With the reduction in the size of the devices to submicron scales it has become a challenge to retain the lattice structure at lower temperatures to avoid undesired diffusion of the dopants [13]. Another method is based on the ion-beam induced epitaxial crystallization (IBIEC) process [3,9,10]. An interesting feature of IBIEC is that this process occurs at temperatures significantly lower than that necessary for SPE [11,12]. It was realized that SPE could also be observed in silicon at temperatures as low as 473–673 K by simultaneous irradiation with energetic ions [14–19]. These studies have adequately demonstrated that the recrystallization process is a consequence of ion-atom

interaction and is not due to the beam heating effects. IBIEC has been explored by various researchers as an alternative method for damage recovery of ion implanted single crystalline materials, especially Si. So far IBIEC has been examined for heavy ions of energies in the range of 1–3 MeV. In contrast to the huge effort performed in the field of ion implantation and irradiation at low energy, very few studies were devoted to the effects of ion bombardment of silicon at higher energies, i.e., in a slowing down regime essentially due to electronic excitations and ionizations, despite the fact that the latter are well known to induce various types of atomic rearrangements in solids. Swift heavy ion beams (100 MeV Ag<sup>7+</sup> and 50 MeV Au<sup>6+</sup> and 100 MeV Au<sup>8+</sup>) were used to study the role of electronic energy loss in ion beam induced epitaxial recrystallization of thin layers of amorphous Si [18,19]. Good epitaxial recrystallization was observed during swift heavy ion beam induced epitaxial crystallization (SHIBIEC) process at 473–623 K which is a much lower temperature as compared to the one needed in SPE growth. In view of all these effects and also for the potential use of Si-based microelectronics in hostile environments it was quite crucial to investigate the behavior of this material under ion irradiation at different energies in order to examine the role of the nuclear collisions and that of the electronic excitations and also to study the possible interference between these two phenomena. For this purpose, Si single crystal samples were irradiated at room temperature separately with low energy 1.345 MeV Au<sup>1+</sup> ions and then with 10 MeV Co<sup>3+</sup> ions and also successively with both ions.

\* Corresponding author at: Horia Hulubei National Institute for Physics and Nuclear Engineering, P.O.B. MG-6, RO-077125, 30 Reactorului St., Magurele-Bucharest, Romania.

E-mail address: [draceamariadiana@gmail.com](mailto:draceamariadiana@gmail.com) (M.D. Mihai).

<https://doi.org/10.1016/j.nimb.2018.09.005>

Received 30 October 2017; Received in revised form 4 September 2018; Accepted 4 September 2018

Available online 12 September 2018

0168-583X/ © 2018 Elsevier B.V. All rights reserved.

## 2. Experimental

Well-polished **Si(1 0 0)** single crystals samples ( $10 \times 10 \text{ mm}^2$ ) were implanted at RT with **1.345 MeV Au<sup>1+</sup>** ions at fluences varied from  **$1 \times 10^{13}$  to  $1 \times 10^{14} \text{ at/cm}^2$** . The calculated values from SRIM2013 code of electronic and nuclear stopping powers ( $S_e$  and  $S_n$ ) are 1.689 and 2.764 keV/nm, respectively, for Au ions in Si. The high nuclear stopping power and a electronic to nuclear ratio of 0.611 are responsible for the displacement damage production in Au irradiated Si. The implantation was performed at the ion-implantation beam line at the 3 MV Tandetron Cockcroft-Walton accelerator of IFIN-HH, which has a raster scanner to scan the beam on the sample for providing uniform implantation over a predefined area. The implantation was performed at an angle of  $7^\circ$  between the sample surface normal and the incident ion beam in an attempt to minimize channeling effects during the implantation. Moreover, in order to minimize target heating during Co irradiation, the ion flux was kept below  $3 \times 10^9 \text{ ions cm}^{-2} \text{ s}^{-1}$ . Different disorder levels were produced for different fluences, with a peak disorder located at a depth of  $\sim 300 \text{ nm}$ . The implanted samples were investigated by Rutherford backscattering spectrometry in channeling geometry using a collimated 2 MeV **He<sup>2+</sup>** beam delivered by the 3 MV Tandetron Cockcroft-Walton accelerator of IFIN-HH at the IBA beam-line. The energy resolution was around 15 keV. Random and aligned spectra were measured.

Previous investigations indicated that ionization effects due to the energy loss to target electrons can anneal pre-existing defects, and therefore may effectively modify or alter microstructure evolution.

In order to check the occurrence of such a phenomenon, we irradiated with **10 MeV Co<sup>3+</sup>** ions at a fluence of  $3 \times 10^{14} \text{ at/cm}^2$  Si crystals previously implanted with 1.345 MeV Au<sup>1+</sup> ions at various fluences between  $1 \times 10^{13}$  and  $1 \times 10^{14} \text{ at/cm}^2$ . Also, a pristine Si crystal was irradiated with 10 MeV Co<sup>3+</sup> ions at the same fluence. The calculated values from SRIM2000 code of  $S_e$  and  $S_n$  are 4.0 and **0.084 keV/nm, respectively, for Co ions in Si**. The Au and Co implanted samples were investigated by RBS/C. The irradiation conditions for different samples are presented in Table 1.

The morphology and local atomic structure were studied using high-resolution transmission electron microscopy (HREM), selected area electron diffraction (SAED) and high resolution X-ray diffraction (HRXRD). TEM studies have been carried out using a JEOL JEM ARM 200F electron microscope operated at 200 kV. The specimens for microscopy have been prepared in both plan-view and cross-section orientations by ion milling at  $7^\circ$  angle of incidence and 4 kV accelerating voltage with a Gatan PIPS installation. Some HREM images were acquired using a Titan Themis image corrected microscope with high brightness XFEG source equipped with an STEM detector, ultrafast EELS spectrometer and a four diode Super-X energy dispersive spectroscopy detector. High resolution X-ray diffraction investigations (HRXRD) were performed with an Empyrean instrument (Panalytical) working with a Cu anode. For high-resolution  $\omega$ - $2\theta$  and  $\omega$  curves, the instrument

**Table 1**  
Irradiation conditions for different samples.

Sample name	1.345 MeV Au fluence	10 MeV Co fluence
1	$1 \times 10^{13} \text{ at/cm}^2$	$3 \times 10^{14} \text{ at/cm}^2$
2	$1 \times 10^{13} \text{ at/cm}^2$	–
3	$3 \times 10^{13} \text{ at/cm}^2$	$3 \times 10^{14} \text{ at/cm}^2$
4	$3 \times 10^{13} \text{ at/cm}^2$	–
5	$5 \times 10^{13} \text{ at/cm}^2$	$3 \times 10^{14} \text{ at/cm}^2$
6	$5 \times 10^{13} \text{ at/cm}^2$	–
7	$7 \times 10^{13} \text{ at/cm}^2$	$3 \times 10^{14} \text{ at/cm}^2$
8	$7 \times 10^{13} \text{ at/cm}^2$	–
9	$1 \times 10^{14} \text{ at/cm}^2$	$3 \times 10^{14} \text{ at/cm}^2$
10	$1 \times 10^{14} \text{ at/cm}^2$	–
11	–	$3 \times 10^{14} \text{ at/cm}^2$
V	Virgin crystal	

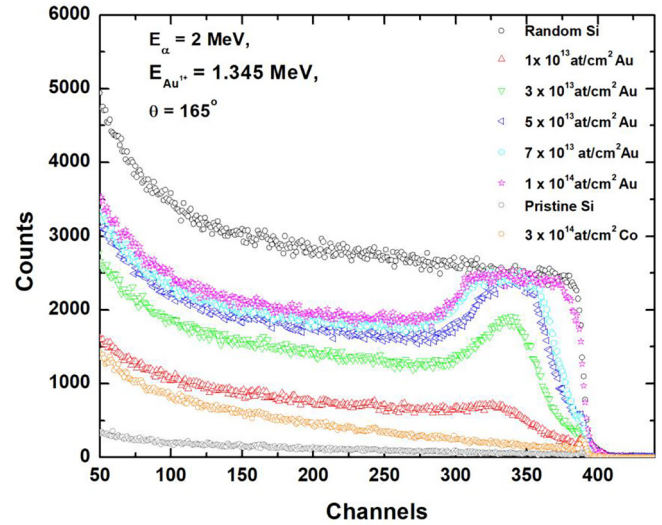


**Fig. 1.** RBS spectra recorded in random and channeling orientations on Si crystals, implanted at RT with 1.345 MeV Au<sup>1+</sup> ions at various fluences between  $1 \times 10^{13}$  and  $1 \times 10^{14} \text{ at/cm}^2$ . The analyzing particles are 2 MeV <sup>4</sup>He ions, at  $\theta = 165^\circ$ .

was set up to work in a parallel beam geometry with a mirror and a 4-bounce channel cut Ge crystal providing monochromatic Cu K $\alpha_1$  radiation in the incident beam side and a 1 mm brass slit and an open proportional detector in the diffracted beam side. The (0 0 4) and (1 1 3) Si peak regions were investigated. The acquired  $\omega$ - $2\theta$  rocking curves were simulated using the Epitaxy software package from Panalytical.

## 3. Results and discussion

Fig. 1 shows the random and aligned RBS spectra from Si single crystal samples implanted with Au ions at different fluences. An aligned RBS spectrum from a pristine Si crystal irradiated with Co ions is also presented. After irradiation with Au ions, the RBS spectra recorded along (1 0 0) axis exhibit a disorder peak which increases with the Au fluence at fluences between  $1 \times 10^{13}$  and  $5 \times 10^{13} \text{ at/cm}^2$ . The sample irradiated with  $5 \times 10^{13} \text{ at/cm}^2$  exhibits a damage peak which reached the random level, indicating the formation of a buried amorphous layer. This fluence for the onset of amorphization is in good agreement with the value reported in Ref. [21]. In order to evaluate quantitatively the evolution of the disorder resulting from the irradiation the RBS spectra were analyzed to extract the damage profile. This analysis was performed by the two-beam approximation [20].

The Au and Co implanted samples were also investigated by RBS/C. Given the low nuclear stopping value and high  $S_e/S_n$  ratio, negligible damage buildup from the nuclear energy deposition within 1  $\mu\text{m}$  of the surface region is expected for the pristine Si crystal implanted with Co ions. This assumption is confirmed as no significant damage buildup is observed on Si lattice along (1 0 0) channeling direction at the fluence used in this study in RBS/C spectrum presented in Fig. 1. One can thus conclude that swift heavy ions are not as efficient as low energy ions for inducing damage in Si. RBS/C spectra recorded in random (black points) and channeling (other symbols) orientations on Si single crystals irradiated at RT with 1.345 MeV Au<sup>1+</sup> at two fluences ( $1 \times 10^{13}$  and  $3 \times 10^{13} \text{ at/cm}^2$ ) and subsequently irradiated at RT with 10 MeV Co<sup>3+</sup> at  $3 \times 10^{14} \text{ at/cm}^2$  are illustrated in Fig. 2. The corresponding disorder profiles are displayed in Fig. 3. The specimen irradiated with  $3 \times 10^{13} \text{ at/cm}^2$  Au gives rise to a crystal nearly half disordered around the Au stopping depth, while the sample irradiated with  $1 \times 10^{13} \text{ at/cm}^2$  gives rise to a rather weakly damaged crystal at the same depth. After Co irradiation one obtains a significant reduction of the amplitude of the damaged region for the sample implanted with Au at a fluence of

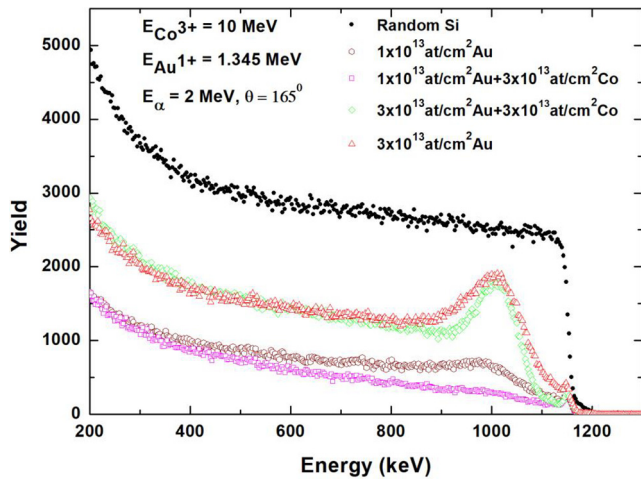


Fig. 2. RBS spectra recorded in random and channeling orientations on Si crystals, previously implanted at RT with 1.345 MeV  $\text{Au}^{1+}$  ions at fluences of  $1 \times 10^{13}$  and  $3 \times 10^{14}$  at/cm<sup>2</sup>, then irradiated at RT with 10 MeV  $\text{Co}^{3+}$  ions at a fluence of  $3 \times 10^{14}$  at/cm<sup>2</sup>. The analyzing particles are 2 MeV  $^4\text{He}$  ions, at  $\theta = 165^\circ$ .

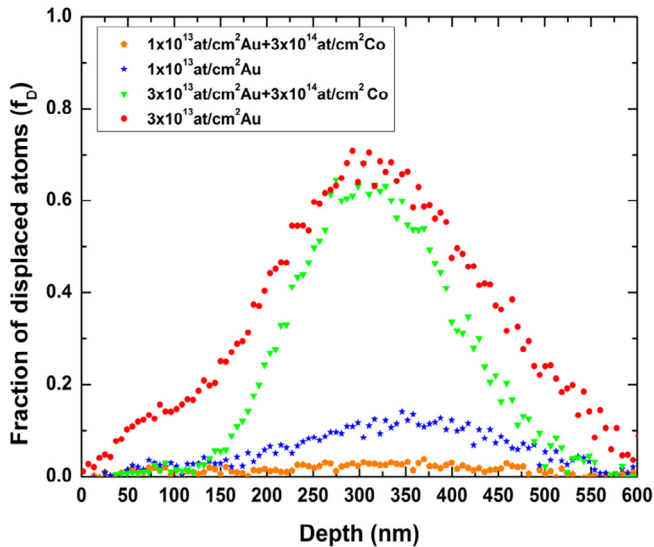


Fig. 3. Damage profiles in the Si crystals, previously irradiated at RT with 1.345 MeV  $\text{Au}^{1+}$  at fluences of  $1 \times 10^{13}$  and  $3 \times 10^{13}$  at/cm<sup>2</sup> respectively and then also irradiated at RT with 10 MeV  $\text{Co}^{3+}$  ions at a fluence of  $3 \times 10^{14}$  at/cm<sup>2</sup>.

$1 \times 10^{13}$  at/cm<sup>2</sup> revealing a clear recrystallization effect. The damage recovery is almost total for the lowest Au fluence used in this study. For the sample implanted with Au at a fluence of  $3 \times 10^{13}$  at/cm<sup>2</sup> one obtains a reduction of the damaged region thickness. The amorphous layer for the sample implanted with Au at  $1 \times 10^{14}$  at/cm<sup>2</sup> fluence starts very close to the surface and has a width  $\sim 500$  nm. For samples implanted at lower fluences the thickness of the amorphised layer decreased up to  $\sim 250$  nm. The subsequent irradiation with Co ions leads to a decrease of the amorphised layers thickness.

In Fig. 4 is presented a HREM image of the lattice planes for a Si sample implanted with Au ions at a fluence of  $5 \times 10^{13}$  at/cm<sup>2</sup>. The image was taken at the surface of the thin film. The amorphous material that can be seen on the bottom of the figure is from resin used at sample preparation. There is a big amount of disorder induced by ion irradiation although the lattice planes are still visible, however containing a high density of defects.

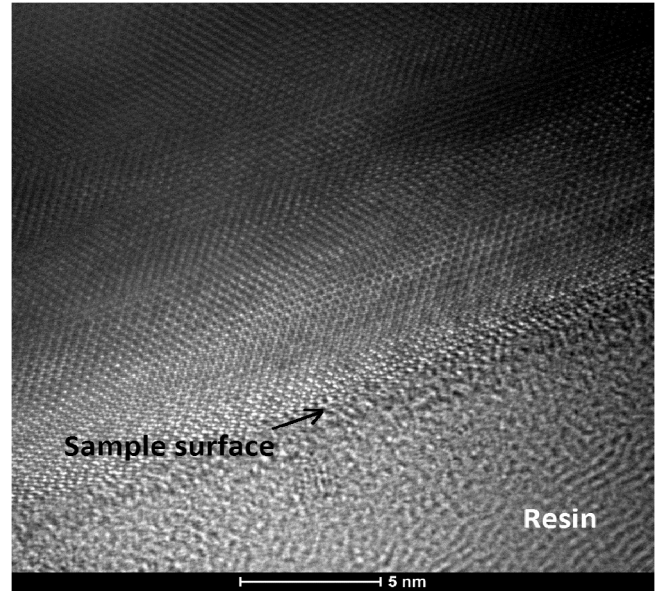


Fig. 4. HREM image of a silicon specimen irradiated with 1.345 MeV  $\text{Au}^{1+}$  ions at a fluence of  $5 \times 10^{13}$  at/cm<sup>2</sup>.

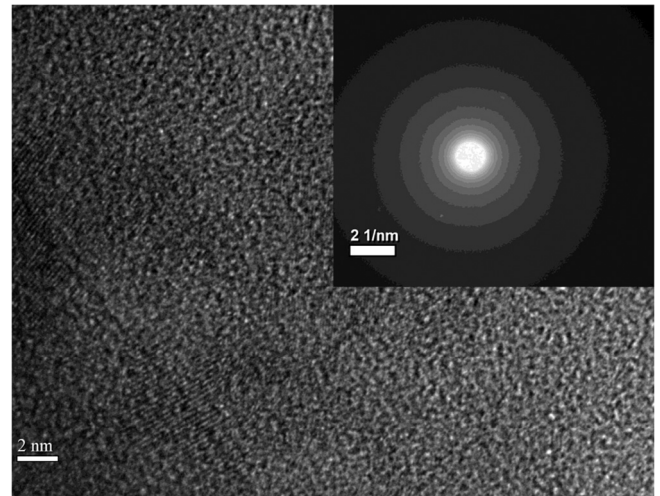
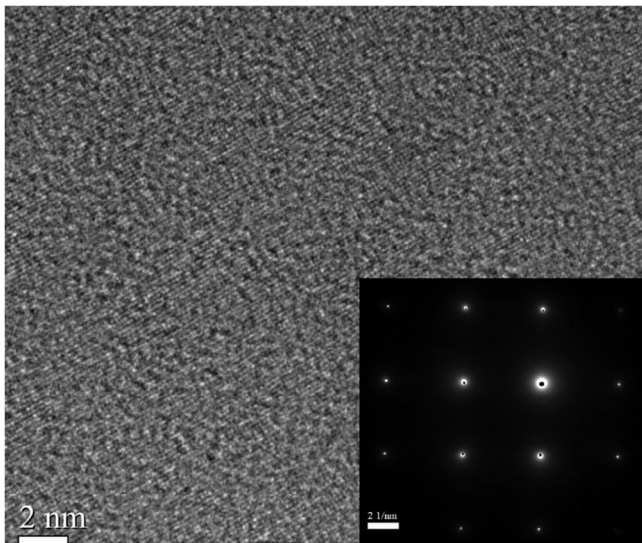


Fig. 5. HREM image of a silicon specimen irradiated with 1.345 MeV  $\text{Au}^{1+}$  ions at a fluence of  $3 \times 10^{13}$  at/cm<sup>2</sup> (the inset is the associated quasiamorphous SAED pattern).

In Fig. 5 it is shown a HRTEM image of a silicon specimen irradiated with 1.345 MeV  $\text{Au}^{1+}$  ions at a fluence  $3 \times 10^{13}$  at/cm<sup>2</sup>. A dominant amorphous structure can be observed, except two areas (lower left side) of about 10 nm diameter where the (220) lattice planes ( $d_{220} = 1.91$  Å) are strongly deformed and crystalline defects are present. The associated SAED pattern (insert Fig. 5) confirms the amorphization process, in agreement with the RBS/C spectrum recorded along the (100) axis which exhibits a disordered peak. For a Si crystal, previously implanted with  $\text{Au}^{1+}$  ions in the above mentioned conditions and finally subjected to an irradiation with 10 MeV  $\text{Co}^{3+}$  ions at a fluence of  $3 \times 10^{14}$  at/cm<sup>2</sup>, a recrystallization effect is evidenced in Fig. 6 by the appearance of lattice planes of {220} type. In insert, a SAED (100) zone axis pattern demonstrates the relative healing of damaged areas.

The samples were further investigated by high resolution X-ray diffraction (HRXRD). In Fig. 7 is presented a comparison of  $\omega$ -2 $\theta$  rocking curves acquired around Si (113) peak from several samples.





**Fig. 6.** HREM image of a silicon specimen irradiated with 1.345 MeV  $\text{Au}^{1+}$  ions at a fluence of  $3 \times 10^{13}$  at/cm<sup>2</sup> and finally with 10 MeV  $\text{Co}^{3+}$  ions at a fluence of  $3 \times 10^{14}$  at/cm<sup>2</sup> (the insert is the corresponding SAED pattern (zone axis 1 0 0)) acquired from the same area).

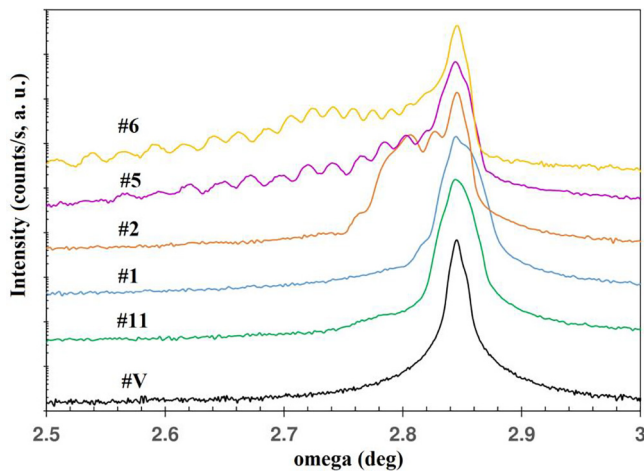


**Fig. 7.** Comparison of  $\omega$ -2 $\theta$  rocking curves recorded around Si (1 1 3) peak from crystals irradiated with 1.345 MeV  $\text{Au}^{1+}$  ions and for crystals irradiated with 10 MeV  $\text{Co}^{3+}$  ions.

The high intensity signal detected at high-angle, observed for a virgin crystal, corresponds also to the scattering of the X-ray beam by the virgin part of the irradiated crystals; the thickness probed by X-rays is larger than the irradiated layer. After irradiation of the samples, new contributions appeared, coming from the damaged part of the crystals. A scattered intensity exhibiting a fringe pattern and corresponding to the implanted layer is visible at lower angles. The fringe spacing shrinks with increasing the gold fluence due to the increase of the damaged region thickness. Sample 2 has the highest concentration of defects and is the most damaged compared with sample 1. There are no thickness fringes visible for sample 1, probably because the damaged layer does no longer have a sharp interface with the underlying Si. The extensive damaged region in samples 1 and 11 disappeared, there are no interference fringes present. However, the Si main peak is wider than the as-received Si peak, there are still a low concentration of defects inside this film. Since the Si (1 1 3) peak is wider in sample 1 than in sample 11, it implies that sample 11 has a higher crystalline quality. The same difference is observed between samples 6 and 5.

Research on ion-solid interactions usually focuses on predicting detrimental effects on materials from particle irradiation, as in nuclear reactors, space applications, and ion-implantation doping of electronic devices. Such destructive effects are often the result of collision cascades induced by low-energy ions. Swift heavy ions (SHIs) have high energies and interact with solids primarily by inelastic collisions with electrons of target atoms. This energy-transfer process results in a state of intense electronic excitations along the ion path that can, particularly in insulating materials, lead to the formation of cylindrical damage regions, commonly referred to as latent ion tracks [22,23], which correspond to permanent structural modifications on the nanometer scale along the ion trajectory. The effect of SHIs on semiconducting materials, on the other hand, is more subtle and significantly less studied. In the present work our aim is not to give a complete interpretation of the results but rather to try to provide keys to explain the behavior of material investigated in this work. Low-energy Au ions which predominantly lose energy through ballistic collisions processes (nuclear energy deposition), induce damage in Si and at higher fluences a phase transformation from crystalline Si (c-Si) to amorphous Si (a-Si) can occur. Understanding the amorphization process is still an active area of research and various mechanisms have been put forward [24–28].

In a figure presenting for all the irradiated samples the relative concentration of displaced Si atoms at the maximum disorder depth versus the Au fluence (not shown here), a sigmoidal dependence of the amorphization buildup is observed. The observed sigmoidal dependence of the amorphization buildup can be interpreted in the framework of a composite amorphization model involving a direct-impact process assisted by a defect stimulated production mechanism [29]. According to this model, at very low fluence each incoming ion creates, within the core of the displacement cascade, an amorphous zone surrounded by a defective crystalline region. In the course of the ion implantation, the volume of the amorphous zones increases due to the accumulation of the direct impact contributions and also due to the overlap of the damage cascades.

The results presented in this work demonstrate that swift heavy ions with energies in the intermediate regime are able to induce an epitaxial recrystallization of the damage created by low energy ion irradiation in silicon. The process occurs at room temperature and does not require the assistance of any external source of heating. The effects described in our work is related to the energy deposited by the incoming Co ions into the target electrons. Such a process can affect drastically the chemistry of the irradiated material due to the huge amount of atomic ionizations and excitations created in the wake of swift ions. It can also lead to a tremendous local transient heating along the ion track according to the so-called “thermal spike” model [30], which is frequently invoked to explain many effects induced by swift heavy ions [31–33]. This phenomenon has been labeled SHIBIEC, which stands for swift heavy ion induced epitaxial recrystallization. Radiation effects in SiC, a wide-band gap semiconductor, have been extensively investigated.

Recently, a significant effect, promoted by the electronic energy loss of ions with energies in the intermediate regime, whereby nearly complete defect annihilation or damage recovery in pre-damaged 4H-SiC is achievable, was reported by Y. Zhang et al [34]. Ionization-induced recovery process in SiC is observed at irradiation conditions as low as 4.5 MeV C, with 21 MeV Ni being the most effective ion beam. High-disorder profiles of  $f_D = 0.72$  and 1.00 are produced using 900 keV  $\text{Si}^{+}$  at fluences of  $6.3 \times 10^{14}$  and  $12 \times 10^{14}$  at/cm<sup>2</sup>, respectively. The relative recovery rate depends on the initial disorder level, and a relatively larger annealing effect is observed for the less-damaged sample ( $f_D = 0.72$ ). For this highly disordered sample, considerable damage recovery is observed after Ni irradiation at ion fluences up to  $3 \times 10^{14}$  at/cm<sup>2</sup>, and the relative disorder decrease from 0.72 to 0.16. At an ion fluence of  $10^{15}$  at/cm<sup>2</sup>, the Si ion-induced damage is almost fully healed; and the ordered atomic structure is confirmed, as shown by the very low disorder level. One can thus assume that such a local

transient heating can, alike conventional thermal treatment, to be able to anneal some structural defects in SiC. Additional experimental and theoretical investigations are, however, necessary in order to get a better insight into the relationship between the ion-induced energy deposition mechanism and the recrystallization process

#### 4. Conclusions

Doping of Si or other semiconductors by ion implantation involves an important step of recovering the damage/amorphization induced by the energetic ions in the lattice. We investigated the damage induced in silicon single crystals due to ion implantation at room temperature of 1.345 MeV Au<sup>1+</sup> ions at fluences from  $1 \times 10^{13}$  to  $1 \times 10^{14}$  at/cm<sup>2</sup>. The ratio  $S_e/S_n$  is 0.611. The fluence for the onset of amorphization was  $\approx 5 \times 10^{13}$  at/cm<sup>2</sup> in good agreement with the value reported in Ref. [21]. A second implantation at room temperature was afterwards performed with 10 MeV Co<sup>3+</sup> ions at a fluence of  $3 \times 10^{14}$  at/cm<sup>2</sup>.

In our combined approach based on ion channeling measurements, high-resolution electron microscopy, selected area electron diffraction and high resolution X-ray diffraction we quantified the effects of electronic energy loss on pre-irradiation-induced lattice damage in Si.

We emphasize to non-negligible recrystallization effects observed in predamaged Si crystals when irradiated with a medium-light ion (Co) with an energy of 10 MeV for which the ratio  $S_e/S_n$  is 47.62.

SHIBIEC does not occur in all materials. It was mainly observed in materials that are weakly damaged by  $S_e$ . The RBS/C spectrum recorded after 10 MeV Co ion irradiation of a pristine Si crystal does not exhibit any significant damage at the fluence used in this study ( $3 \times 10^{14}$  at/cm<sup>2</sup>). RBS/C measurements show that the damage recovery is almost total in the sample implanted at the lowest Au fluence and then irradiated with 10 MeV Co ions. The damage region seen on HRXRD curves on the same sample disappeared after irradiation with Co ions in good agreement with the RBS/C results. For samples implanted with Au at higher fluences a decrease of the thickness of the amorphous layer was observed after Co irradiation.

Additional experimental and theoretical investigations are, however, necessary in order to get a better insight into the relationship between the ion-induced energy deposition mechanism and the recrystallization process.

The ionization-induced annealing process (recovery of the ordered atomic structure) in Si has a significant impact on low-temperature processes for eliminating defect production during ion-implantation doping, suppression of single-event upset damage in Si devices, enhanced radiation tolerance and reliable performance prediction for materials in extreme radiation environments.

#### References

- [1] J.S. Williams, *Surface Modification and Alloyings by Laser Ion and Electron Beams*, Plenum Press, New York, 1983.
- [2] A. Kinomura, et al., *Nucl. Instr. Meth. B* 148 (1999) 370.
- [3] J. Linnros, et al., *Phys. Rev. B* 30 (1984) 3629.
- [4] J.S. Williams, et al., *Phys. Rev. Lett.* 55 (1985) 1482.
- [5] J. Nakata, *Phys. Rev. B* 43 (1991) 14643.
- [6] J. Nakata, *J. Appl. Phys.* 79 (1996) 682.
- [7] L. Csepregi, et al., *Appl. Phys. Lett.* 29 (1976) 645.
- [8] C.J. McHargue, J.M. Williams, *Nucl. Instr. Meth. Phys. Res. B* 80/81 (1993) 889.
- [9] I. Golecki, et al., *Phys. Lett.* 71A (1979) 267.
- [10] J. Nakata, et al., *Jpn. J. Appl. Phys.* 20 (1981) 2211.
- [11] V. Heera, et al., *J. Appl. Phys.* 77 (1995) 2999.
- [12] V. Heera, et al., *Appl. Phys. Lett.* 67 (1995) 1999.
- [13] J. Conrad, Ph.D. thesis, Universität Göttingen, 1996, unpublished.
- [14] R.S. Walker, D.A. Thompson, *Nucl. Instr. Meth.* 135 (1976) 489.
- [15] V. Heera, T. Henkel, R. Kögler, W. Skorupa, *Phys. Rev. B* 52 (1995).
- [16] G. Lulli, P.G. Merli, M.V. Antisari, *Phys. Rev. B* 36 (1987) 8038.
- [17] G.H. Vineyard, *Radiat. Eff. Defects Solids* 29 (1976) 254.
- [18] P.K. Sahoo, et al., *Nucl. Instr. Meth. B* 240 (2005) 239.
- [19] P.K. Sahoo, et al., *Nucl. Instr. Meth. B* 257 (2007) 244.
- [20] W.K. Chu, J.W. Mayer, M.-A. Nicolet, *Backscattering Spectrometry*, Academic, New York, 1978.
- [21] J. Kamila, et al., *NIM B* 207 (2003) 291–295.
- [22] R.L. Fleischer, P.B. Price, R.M. Walker, *Science* 149 (1965) 383.
- [23] M. Toulemonde, W. Assmann, C. Dufour, A. Meftah, F. Studer, C. Trautmann, *Mat. Fys. Medd.* 52 (2006) 263.
- [24] F.F. Morehead Jr., B.L. Crowder, *Radiat. Eff.* 6 (1970) 27.
- [25] M.L. Swanson, J.R. Parsons, C.W. Hoelke, *Radiat. Eff.* 9 (1971) 249.
- [26] O.W. Holland, S.J. Pennycook, G.L. Albert, *Appl. Phys. Lett.* 55 (1989) 2503.
- [27] T. Motoka, S. Harada, M. Ishimaru, *Phys. Rev. Lett.* 78 (1997) 2980.
- [28] K.-M. Wang, F. Chen, H. Hu, J.-H. Zhang, X.-D. Liu, D.-Y. Shen, T. Narusawa, M. Nagaki, *Jpn. J. Appl. Phys.* 41 (2002) 918.
- [29] N. Hecking, K.F. Heidemann, E. te Kaat, *Nucl. Instr. Meth. Phys. Res. B* 15 (1986) 760.
- [30] F. Seitz, J.S. Koehler, *Solid State Phys.* 2 (1956) 305.
- [31] H. Trinkaus, A.I. Ryazanov, *Phys. Rev. Lett.* 74 (1995) 5072.
- [32] A. Benyagoub, *Phys. Rev. B* 72 (2005) 094114.
- [33] S. Klumünzer, *Nucl. Instr. Meth. Phys. Res. B* 244 (2006) 1.
- [34] Y. Zhang, et al., *Nat. Commun.* 6 (2015) 8049, <https://doi.org/10.1038/ncomms9049>.